The melting temperature of molecular nanocrystals at the lower bound of the mesoscopic size range

2000 J. Phys.: Condens. Matter 12 8819

(http://iopscience.iop.org/0953-8984/12/41/307)

J. Phys.: Condens. Matter **12** (2000) 8819–8824. Printed in the UK PII: S0953-8984(00)14849-0

The melting temperature of molecular nanocrystals at the lower bound of the mesoscopic size range

Z Wen, M Zhao and Q Jiang†

Department of Materials Science and Engineering, Jilin University of Technology, Changchun 130025, China

E-mail: jiangq@post.jut.edu.cn (Q Jiang)

Received 20 June 2000

Abstract. Our simple thermodynamic model, free of any adjustable parameters, has predicted the size-dependent and dimension-dependent melting temperatures of molecular nanocrystals whose diameters are at the lower bound of the mesoscopic size range, of 2 to 10 nm. In this size range, the depression of the melting temperature is no longer proportional to the reciprocal of the diameter of the nanocrystals. The model predictions are supported by experimental and molecular dynamics simulation results for cyclohexane, benzene, *n*-decane, methyl chloride, oxygen, neon, argon, and krypton nanocrystals.

It is well known that all low-dimensional crystals, including metallic [1–4], semiconductor [5], and organic [6, 7] particles, nanowires, and thin films, melt below their bulk melting temperatures due to the large surface-to-volume ratio when the surfaces of the crystals are free or without strong chemical interaction with contacted substrates. The melting point depression of the materials is roughly proportional to the reciprocal of their diameter D [1, 5, 8]. However, when D approaches the lower bound of the mesoscopic size range, a deviation from the above proportionality arises. For comparison, we first discuss the classical relationship between the melting temperature and the diameter of the crystals. The melting of small nanocrystals has been described by three kinds of model [8]: (1) the homogeneous melting model without a liquid skin; (2) the liquid-skin melting model; (3) the liquid nucleation and growth model with an unstable liquid skin. All three models predict a size-dependent melting temperature $T_m(D)$ that varies inversely with D. If γ is the interfacial energy per unit area, and subscripts s, l, and v identify the solid, liquid, and vapour phases, respectively, for most cubic metals we have [8]

$$\gamma_{sv} - \gamma_{lv} \approx \gamma_{sl}. \tag{1}$$

When equation (1) is appropriate (this should be true for quasi-isotropic nanocrystals), all of the above three kinds of model predict essentially the same $T_m(D)$ function [8]:

$$T_m(D)/T_m(\infty) = 1 - 4V_s\gamma_{sl}/[H_m(\infty)D] \tag{2}$$

where $H_m(\infty)$ denotes the molar bulk melting enthalpy, $T_m(\infty)$ is the bulk melting temperature, V_s is the molar volume of the crystal. In fact, Pawlow established a version of equation (2) in 1909 which is expressed as [9]

$$T_m(D)/T_m(\infty) = 1 - 4V_s[\gamma_{sv} - \gamma_{lv}(\rho_s/\rho_l)^{2/3}]/[H_m(\infty)D] \tag{3}$$

† Author to whom any correspondence should be addressed. Telephone: +86-431-5705371; fax: +86-431-5687607.

0953-8984/00/418819+06$30.00

where ρ_s and ρ_l are the densities of the solid and the liquid. Since $\rho_s \approx \rho_l$, $(\rho_s/\rho_l)^{2/3} \approx 1$. Considering equation (1), equation (3) $\approx$ equation (2) is obtained. Because γ_{sl} is difficult to measure [10, 11], γ_{sl} has been deduced according to the Gibbs–Thomson equation [10]:

$$\gamma_{sl} = 2hS_{vib}(\infty)H_m(\infty)/(3V_sR) \tag{4}$$

with $S_{vib}(\infty)$ being the vibrational contribution of the overall melting entropy of the bulk crystals and R the ideal-gas constant. Substituting equation (4) into equation (2),

$$T_m(D)/T_m(\infty) = 1 - 8hS_{vib}(\infty)/(3RD). \tag{5}$$

Although equation (5) is in good agreement with the experimental data when $D \geqslant 10$ nm, it fails for nanocrystals with $D < 10$ nm and cannot explain a dimension-dependent $T_m(D)$ (later it will be found that equation (5) is a special case in our model for nanowires when D is larger than 10 nm [2–4]).

Recently, a model, free of any adjustable parameters, for the size-dependent and dimension-dependent melting temperature $T_m(D)$ was introduced in terms of Lindemann's criterion for melting [2–4] and the expression of Mott for $S_{vib}(\infty)$ at $T_m(\infty)$ [18, 19] takes the following form [2–4, 7]:

$$T_m(D)/T_m(\infty) = \exp\{-2S_{vib}(\infty)/[3R(D/D_0 - 1)]\} \tag{6}$$

where D_0 denotes a critical diameter at which all atoms of the nanocrystals are located on its surface. D_0 depends on the dimension of the crystal d: $d = 0$ for nanocrystals, $d = 1$ for nanowires, and $d = 2$ for thin films. For a nanoparticle, D has the usual meaning of the diameter. For a nanowire, D is taken as its diameter. For a thin film, D denotes its thickness. Let h be the atomic diameter; D_0 is given by [2–4]

$$D_0 = 2(3 - d)h. \tag{7}$$

Since a crystal is characterized by its long-range order, the smallest nanocrystal should have at least half of the atoms located within the nanocrystal. Hence, the smallest D is $2D_0$ [2, 3]. This estimate is consistent with experimental results for Bi film [20] and Pb nanowire in a carbon nanotube [21]. Equation (6) has predicted the size-dependent melting for nanoparticles [17], thin films [3], and nanowires [2, 7]. The available experimental evidence confirms the predicted results. In fact, $2D_0$ is about the lower size bound for nanocrystals, being about 2 nm when $h = 1/3$ nm. Since each molecule in a molecular crystal consists of, at least, two atoms (except for rare gas), which occupy one site in the crystal lattice, h given above is defined as the nearest-neighbour separation of molecules in the molecular lattice. Since the vibrational contribution to the melting entropy is essential for molecular crystals, $S_{vib}(\infty) \approx S_m(\infty)$ [7] is taken in all later calculations.

Note that in view of the mathematical relationship $e^{-x} \approx 1 - x$ holding under the condition that D is much larger than D_0,

$$T_m(D)/T_m(\infty) = 1 - 2D_0S_{vib}(\infty)/(3RD). \tag{8}$$

Let equation (8) = equation (5); we get $D_0 = 4h$. Thus, the correspondence between our model and previous models is realized when the middle dimension of $d = 1$ is taken and D is large enough. However, when $d \neq 1$ and D is small, such as at the lower bound of the mesoscopic size range, there is a difference between equation (8) and equation (5), which will be observed in the following figures.

Molecular nanocrystals can be obtained by using the corresponding liquids to fill porous materials, such as MCM-41 [6, 13, 22]. The pores are of cylindrical-like nature, arranged parallel in a honeycomb-type lattice [13]. Therefore, $d = 1$ and $D_0 = 4h$ from equation (7). The calculated values of h are listed in table 1.

Table 1. Determination of h and corresponding lattice parameters, symmetries, and numbers per unit cell.

Substance	Symmetry	Lattice parameter (nm)	Molecular numbers per unit cell	Determination of h (nm)
Cyclohexane [23]	Cubic	$a = 0.861$	4	$h = \sqrt{2}a/2 = 0.6088$
Benzene [14]	Orthorhombic	$a = 0.740$ $b = 0.953$ $c = 0.692$	4	$h = \sqrt{a^2 + c^2}/2 = 0.5066$
n-decane [16]	Triclinic	$a = 0.425$ $b = 0.4805$ $c = 1.481$	1	$h = a = 0.425$
Methyl chloride [13]	Orthorhombic	$a = 0.6495$ $b = 0.5139$ $c = 0.7523$	4	$h = \sqrt{a^2 + b^2}/2 = 0.4141$
Oxygen [15]	Cubic	$a = 0.4457$ $b = 0.3323$ $c = 0.5076$	4	$h = \sqrt{a^2 + b^2}/2 = 0.5560$

The functions $T_m(D)$ for four organic molecular nanocrystals have been calculated using equation (6) and are shown in figures 1 and 2, where the $T_m(D) \sim 1/D$ relationship based on equation (5) is also shown for comparison purposes. In addition, figures 1 and 2 show the experimental observations [6, 13, 23, 24] and the results of molecular dynamics (MD) simulations [23, 24]. It is evident that the model prediction is consistent with the experimental observation and the results of the MD simulation where the melting temperature decreases with decrease in size. However, all drops in the melting temperatures differ from a straight when $D < 8$ nm as the figures show, although equations (5) and (6) give almost the same

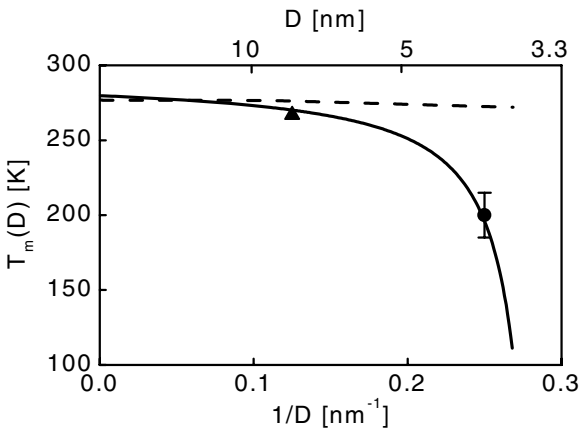

Figure 1. The function $T_m(D)$ for cyclohexane nanocrystal. The solid line is the theoretical prediction from equation (6). ● denotes the MD result [23] and ▲ the experimental result [24] for $T_m(r)$ for porous spherosils. The corresponding values of $T_m(\infty)$ and $S_m(\infty)$ are 279.82 K [25] and 0.5311 J K^{-1}/(g atom) [11]. $D_0 = 6h = 3.652$ nm from equation (7), where $h = 0.6088$ nm. The straight dashed line is obtained from equation (5).

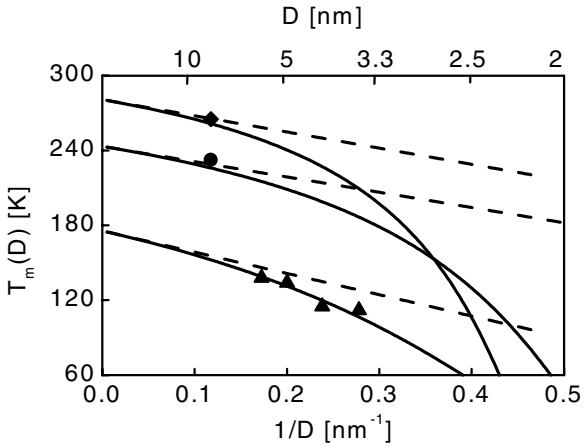

Figure 2. The functions $T_m(D)$ for benzene, decane, and methyl chloride nanocrystals. The solid lines are the model predictions of equation (6). ♦, ●, and ▲ denote the experimental values of $T_m(D)$ for benzene [6], n-decane [6], and methyl chloride [13] in a single cylindrical pore, respectively. The values of $T_m(\infty)$ for benzene, n-decane, and methyl chloride (in K) are 280.8, 243.3 [6], and 175.6 [13], respectively. The corresponding values of $S_m(\infty)$ (in J K^{-1}/(g atom)) are 2.842, 3.693 [6], and 7.317 [11]. $D_0 = 4h$ (in nm) takes the values 2.026, 1.700, and 1.6564. The straight dashed lines are is obtained from equation (5).

results when $D > 10$ nm. Note also that the relative drop of the melting point depends on the relative size of D_0. Since D_0 for cyclohexane in figure 1 is about two times those for other molecules in figure 2 due to the differences of both h and d, a stronger drop of the melting temperature is observed.

Figures 3 and 4 give the experimental and MD results for four nanocrystals of gas molecules. The corresponding theoretical predictions from equations (5) and (6) are also

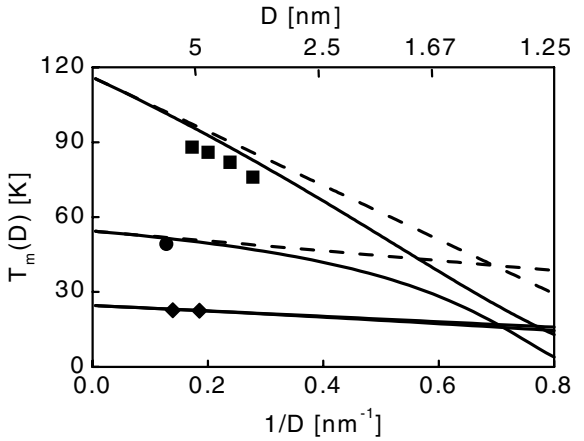

Figure 3. The functions $T_m(D)$ for krypton, oxygen, and neon. The solid lines are model predictions based on equation (6). ■, ●, and ♦ denote the experimental values of $T_m(D)$ for krypton [22], oxygen [25], and neon [25, 26], respectively. The corresponding values of $T_m(\infty)$ (in K) are 116.0 [22], 54.4 [25], and 24.6 [25, 26], and the values of $S_m(\infty)$ (in J K^{-1}/(g atom) are 14.14 [22], 4.073 [11], and 13.54 [12]. $D_0 = 4h$ (in nm) takes the values 0.824, 1.112, and 0.408. The straight dashed lines are obtained from equation (5).

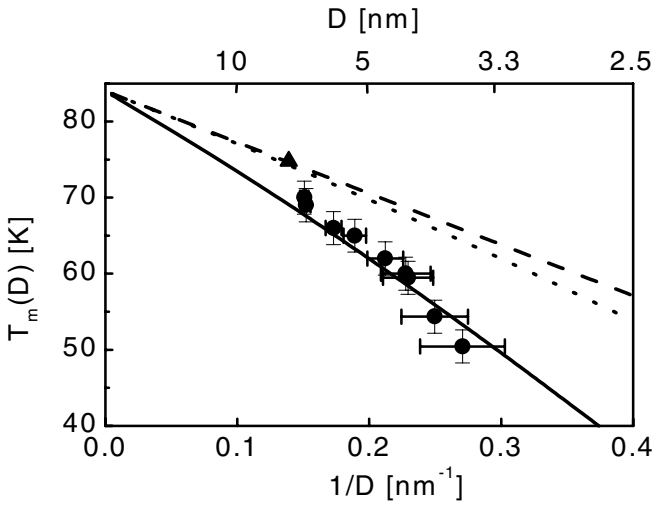

Figure 4. The function $T_m(D)$ for argon. The solid and dashed lines are model predictions from equation (6) for nanoparticles ($D_0 = 6h = 1.056$ nm) and nanowire ($D_0 = 4h = 0.704$ nm) confined in porous glasses where $h = 0.176$ nm [12], and $S_m(\infty) = 14.18$ J K^{-1}/(g atom) [12]. ● and ▲ denote the values of $T_m(D)$ from MD simulations for Ar nanoparticles [27] and experimental values of $T_m(D)$ for Ar nanowires [25]. The straight dotted line is obtained from equation (5).

present in the figures. Although the chemical bonds of organic molecules and gas molecules are different, the same model, equation (6), can describe their size dependences on the melting points. Here we again find that equation (5) fails to predict the experimental results when D is smaller than about 8 nm while our model can do that for the full size range from the lower bound of the mesoscopic size range of about 2 nm to the macroscopic size range. Note that figure 4 presents further the influence of the dimension, where $d = 1$ and $d = 2$ have been used for nanowires and thin films, respectively. It is clear that equation (5) in fact corresponds to $d = 1$ within our model, which confirms the above discussion as regards the relationship between equation (5) and equation (6). When the size of the nanocrystals is lower than about 8 nm, the difference between $T_m(D)$ for $d = 1$ and that for $d = 2$ becomes evident. Thus, the values of $T_m(D)$ for molecular nanocrystals do indeed depend on the dimension of the nanocrystals. A lower dimension of the crystal leads to a larger value of ΔT—i.e., for the same substance at the same D, a particle has a larger thermodynamic undercooling than a nanowire, as shown in figure 4. This difference comes from the different ratios between the surface molecules and the interior molecules in different dimensions.

All of the above results indicate that the difference of equations (5) and (6) becomes evident since the molecular percentage of surface molecules is more than 20% when the crystals have dimension $D < 8$ nm. This large percentage leads to the linear relationship between $T_m(D)$ and $1/D$, as the first-order approximation, failing.

In conclusion, molecular nanocrystals exhibit reduced melting temperature with decreasing crystal size since the vibrational spectrum of the surface region differs from that of the bulk. Equation (6) not only clearly gives the same description of the $T_m(D) \sim 1/D$ relationship when $D > 10$ nm, but also does this when the size of the nanocrystals decreases to the lower bound of the mesoscopic size range, about 2 nm. The model predictions are supported by available experimental observations for molecular nanocrystals and by molecular dynamics simulation results.

Acknowledgments

The financial support of the National Natural Science Foundation of China under Grant No 59931030 and the Trans-Century Training Programme Foundation for Talents of the Ministry of Education of China are acknowledged.

References

[1] Hasegawa M, Hoshino K and Watabe M 1980 *J. Phys. F: Met. Phys.* **10** 619
[2] Jiang Q, Aya N and Shi F G 1997 *Appl. Phys.* A **64** 627
[3] Jiang Q, Tong H Y, Hsu D T, Okuyama K and Shi F G 1998 *Thin Solid Films* **312** 357
[4] Jiang Q and Shi F G 1998 *Mater. Lett.* **37** 79
[5] Goldstein A N, Ether C M and Alivisatos A P 1992 *Science* **256** 1425
[6] Jackson C L and McKenna G B 1990 *J. Chem. Phys.* **93** 9002
[7] Jiang Q, Shi H X and Zhao M 1999 *J. Chem. Phys.* **111** 2176
[8] Peters K F, Cohen J B and Chung Y W 1998 *Phys. Rev.* B **57** 13 430
[9] Pawlow P 1909 *Z. Phys. Chem.* **65** 545
[10] Jiang Q, Shi H X and Zhao M 1999 *Acta Mater.* **47** 2109
[11] Dean J A 1985 *Lange's Handbook of Chemistry* 13th edn (New York: McGraw-Hill) pp 9-107–9-160
[12] *Table of Periodic Properties of the Elements* 1980 (Skokie, IL: Sargent-Welch Scientific Company) p 1
[13] Morishige K and Kawano K 1999 *J. Phys. Chem.* B **103** 7906
[14] *The Joint Committee on Powder Diffraction Standards* PDF 10-800
[15] *The Joint Committee on Powder Diffraction Standards* PDF 45-912
[16] *The Joint Committee on Powder Diffraction Standards* PDF 30-1685
[17] Shi F G 1994 *J. Mater. Res.* **9** 1307
[18] Mott N F 1934 *Proc. R. Soc.* A **146** 465
[19] Regel' A R and Glazov V M 1995 *Semiconductors* **29** 405
[20] Mitch M G, Chase S J, Fortner J, Yu R Q and Lannin J S 1991 *Phys. Rev. Lett.* **67** 875
[21] Ajayan P M and Iijima S 1993 *Nature* **361** 233
[22] Morishige K and Kawano K 2000 *J. Phys. Chem.* B **104** 2894
[23] Celestini F, Pellenq R J-M, Bordarier P and Rousseau B 1996 *Z. Phys.* D **37** 49
[24] Mu R and Malhotra V M 1991 *Phys. Rev.* B **44** 4296
[25] Molz E, Wong A P, Chan M H W and Beamish J R 1993 *Phys. Rev.* B **48** 5741
[26] Tell J and Maris H J 1983 *Phys. Rev.* B **28** 5122
[27] Trew A S, Pawley G S and Cairns-Smith A 1990 *Acta Crystallogr.* A **46** 979